Protein-nanoparticle complex structure determination by cryo-electron microscopy

Sagnik Sen[a,b,1], Amar Thaker[a,b,1], Luqmanal Sirajudeen[a,b], Dewight Williams[c], Brent L. Nannenga[a,b,*]

[a]Chemical Engineering, School for Engineering of Matter, Transport and Energy, Arizona State University, Tempe, AZ, USA

[b]Biodesign Center for Applied Structural Discovery, Biodesign Institute, Arizona State University, 727 East Tyler Street, Tempe, AZ 85287, USA

[c]John M. Cowley Center for High Resolution Electron Microscopy, Arizona State University, Tempe, AZ, USA

[1]These authors contributed equally to this work

[*]corresponding author: brent.nannenga@asu.edu

Abstract

Methods that allow the study of the structure of proteins in complex with nanomaterials promise to enhance our understanding of how biological molecules interface with inorganic materials. We used single particle cryo-EM to demonstrate the potential for cryo-EM analysis to reveal structural details of protein-nanoparticle complexes. Two protein nanomaterial complexes, GroEL bound to platinum nanoparticles (GroEL-PtNP), and ferritin bound to an iron oxide nanoparticle were used as model samples. For the GroEL-PtNP complex, a final reconstruction was obtained to 3.93Å, which allowed the atomic model of GroEL to be fit into the resulting map. This sets the stage for future work and improvements on the use of cryo-EM for the study of protein-nanomaterial complexes.

Keywords

Cryo-electron microscopy, single particle cryo-EM, nanomaterials, biomineralization, protein structure

Main Text

Due to their tunable size, shape, and composition, nanomaterials exhibit a variety of unique properties (e.g. electronic, optical, and magnetic properties), which are leading to innovative applications in such diverse fields as energy storage, medicine, catalysis, composite materials, and advanced imaging technologies [1-3]. Both natural [4-7] and engineered [8-14] biological systems are capable of directing the synthesis and formation of inorganic nanomaterials with exquisite control over size, shape and function [12, 15-17]. Elucidating the molecular processes responsible for biological control of material synthesis is critical to our fundamental understanding of the mechanisms that biology uses to interact with and shape the inorganic world. Determining the interactions at the interface between biological molecules and inorganic surfaces is essential for ultimately harnessing the power of biological molecules to synthesize novel materials and hybrid nanobiomaterials.

Currently, there are very limited high-resolution structures of biological molecules directly interacting with an inorganic nanomaterial [18], and much of our understanding comes from surface binding studies, or studies using computer simulations [19-23]. The most widely used structure determination methods, X-ray crystallography and solution state nuclear magnetic resonance (NMR), are not ideal for solving the structures of biological molecules materials bound to inorganic surfaces[18, 24]; therefore, the application of other methods is of great interest. Techniques such as solid state NMR[24, 25] and sum frequency generation (SFG) vibrational spectroscopy[18, 26] have been used to successfully analyze the interaction of smaller biomineralizing proteins interacting with inorganic substrates. However, despite providing very informative data, these methods are currently limited to small proteins, and many complementary techniques are required to interpret the structural data[18, 24, 26, 27]. The field of biomineralization and the study of the biomolecule-inorganic material interface would greatly benefit from complimentary and improved structural analysis methods. In recent years, cryo-electron microscopy (cryo-EM) has revolutionized the

field of structural biology, and in this work, we sought to demonstrate the use of single particle cryo-EM methods to the analysis of protein-nanomaterial complexes. In the case of a model GroEL and platinum nanoparticle (PtNP) system we show that cryo-EM can be used to determine high-resolution structures of proteins and nanomaterials.

The first model system we chose to apply cryo-EM to was GroEL bound to PtNPs. GroEL is a 60 kDa protein that assembles into homo-tetradecameric complex consisting of two stacked heptameric rings[28]. Together with GroES, GroEL aids in the folding of many proteins within the central cavity of the complex and is essential for cell viability [29]. In addition to the essential roles of GroEL in protein folding, it has been shown that GroEL can aid in the synthesis of stable PtNPs when added to a solution of K_2PtCl_4 that is then reduced by $NaBH_4$[30], and that the PtNPs are associated with GroEL. In this work, we used similar procedures and to produce GroEL-PtNP complexes with the goal of analyzing their structure by single particle cryo-EM. GroEL overexpression in *E. coli* was controlled by a T7 expression vector, and cells were induced with IPTG overnight at 25°C. Following expression, cells were harvested, lysed by sonication, and purified by ammonium sulfate precipitation followed by size exclusion chromatography (see SI for detailed protocols). PtNPs were synthesized by reduction of a mixture of 2 mM K_2PtCl_4 with 15 mM $NaBH_4$ in the presence of 5 μM GroEL. After incubation for 2 hours, the solution was a homogenous brown color indicating the formation of PtNPs (Fig 1A). Following PtNP synthesis, the GroEL-PtNP sample was deposited on holey carbon grids and vitrified for cryo-EM analysis. Cryo-EM data were collected on a Titan Krios equipped with a K2 summit direct electron detector in counting mode. Initial images of the particles showed many PtNPs near GroEL proteins, and many of the GroEL proteins contained PtNPs within the central cavity of the GroEL complexes (Fig 1B). A data set of 2,730 movies were collected on the GroEL-PtNP samples and the movie frames were motion corrected using MotionCor2[31]. Following motion correction, the cryo-EM data processing software package cisTEM[32] was used for further data processing. Initially 182,527

particles were extracted from the images and subjected to two rounds of 2D classification where high-quality classes containing clear PtNPs, consisting of 52,409 particles were selected. Following 2D classification, ab initio 3D reconstruction and refinement were performed, and final maps were sharpened without masking in cisTEM using the default values of -90.00 $Å^2$ and 0.00 $Å^2$ for Pre-cut-off and Post-cut-off B-factors, respectively.

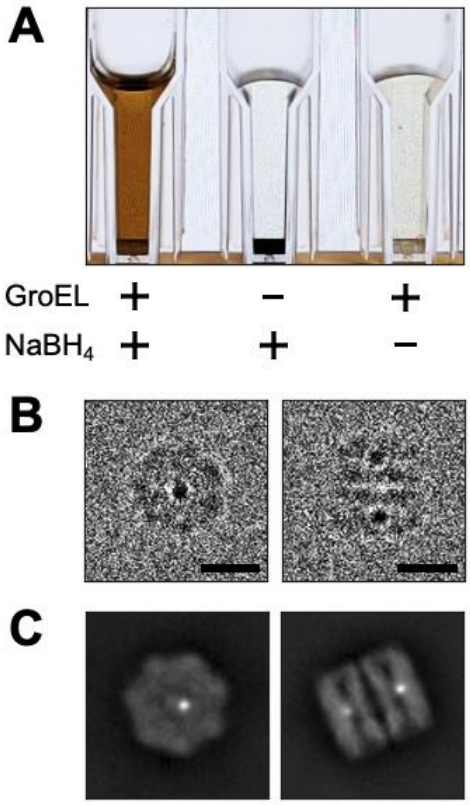

Figure 1. Synthesis of GroEL-PtNP nanoparticles. (A) When the solution of GroEL and K_2PtCl_4 is reduced by $NaBH_4$, the solution becomes a homogenous light brown in color, indicating the formation of PtNPs, and these nanoparticles remain in solution without settling. In the absence of GroEL, stable nanoparticles are not formed but rather a black precipitate that settles to the bottom of the container. (B-C) Representative GroEL particles (B) and 2D classes (C) that contain PtNP within the central cavity of the protein assembly. Scale bar in B represents 10 nm.

GroEL has D7 symmetry; however, it was unclear how the PtNPs in the central cavity would impact the overall symmetry. Therefore, the initial reconstruction of the GroEL-Pt complexes was performed without applying any symmetry. In this first unsymmetrized structure there is a nanoparticle present in both heptameric rings of GroEL (Fig S2). This indicated that while the

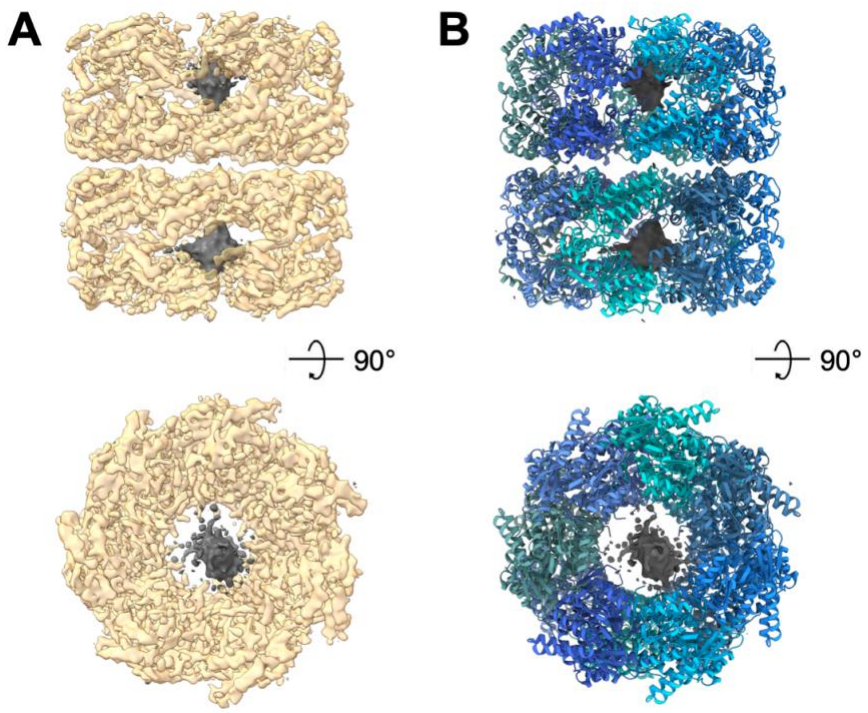

Figure 2. Structure of GroEL-PtNPs. (A) The final 3.93Å reconstruction of GroEL (gold) with PtNPs (gray) in the central cavity resulted from 52,409 particles and the application of C2 symmetry. (B) The quality of map obtained allowed the atomic model of GroEL (PDB ID: 1ss8) to be placed within the map and the relative orientation of the PtNPs to the protein could be identified.

location of the PtNP broke the 7-fold symmetry of GroEL, the 2-fold symmetry between the heptameric rings could still be applied. Therefore, we used C2 symmetry in subsequent reconstructions and achieved an improvement in resolution to 3.93Å (Fig 2; S3). This higher resolution map allowed us to place the atomic model for GroEL within the density map and identify the relative orientation of the nanoparticle within the protein core. In the model, the closest part of GroEL to the PtNP is the α-helix formed by residues G256 to R268 (Fig. S4), and the nanoparticle is near two of these helices from two adjacent monomers. Interestingly in the model R268 extends towards the nanoparticle, however, the present maps are not of sufficient resolution in this region to determine the conformation of these arginine residues in the presence of the PtNP unambiguously. Future work will seek to understand the role of these helices in the interaction between GroEL and PtNPs.

The above structure of GroEL-PtNP was obtained using the standard single particle cryo-EM workflow as implemented within cisTEM. To investigate whether other protein-nanomaterial complexes could also be analyzed by standard cryo-EM procedures we next used human light chain ferritin complexed with iron oxide nanoparticles (HuLF-FeNP). Ferritins are a class of biomineralizing proteins composed of 24 subunits that assemble into a highly symmetric nanocage approximately 12 nm in diameter, with an 8 nm hollow core where iron oxide mineralization occurs [33]. Ferritins play a critical role maintaining iron levels within cells, and several debilitating diseases and disorders produce altered levels of ferritin in the body [34]. In addition to its critical role in maintaining iron homeostasis, ferritin has seen numerous applications in biotechnology [35], including directed synthesis of a semiconductor materials [36, 37], exploiting the magnetic properties of iron oxide loaded ferritin for MRI [38], and biomolecule-based water purification systems [39]. Recombinant Human light chain ferritin (HuLF) was expressed and purified, and the formation of iron oxide within the ferritin was performed as described previously [40]. Briefly, HuLF was expressed in *E. coli*, and purified by ammonium sulfate precipitation followed by size exclusion chromatography. Purified HuLF was then incubated with a low amount of ammonium iron(II) sulfate (HuLF subunit to Fe^{2+} ratio of 1:3) for 4 hours. The low ratio HuLF:Fe^{2+} was selected to encourage the formation of single nanoparticles within each ferritin complex. The reaction mixture was then passed through a desalting column to remove excess iron, and cryo-EM samples were applied to holey carbon grids and vitrified for single particle analysis. From this sample, 2,740 movies of HuLF-FeNPs were collected and processed in cisTEM. Briefly, 145,032 particles were selected and subjected to three rounds of 2D classification. Classes with nanoparticles within ferritin were selected for 3D ab initio reconstruction and refinement using cisTEM. As with the GroEL-PtNPs sample, the initial reconstructions of HuLF-FeNPs were performed with no symmetry applied. Unfortunately, in the case of HuLF-FeNPs, the resolution was significantly lower and clear secondary structure could not be resolved in these maps. While

these maps did not allow an accurate fitting of the atomic model for HuLF, the iron oxide nanoparticle could be located on the inner surface of the HuLF shell in the lower resolution maps (Fig 3).

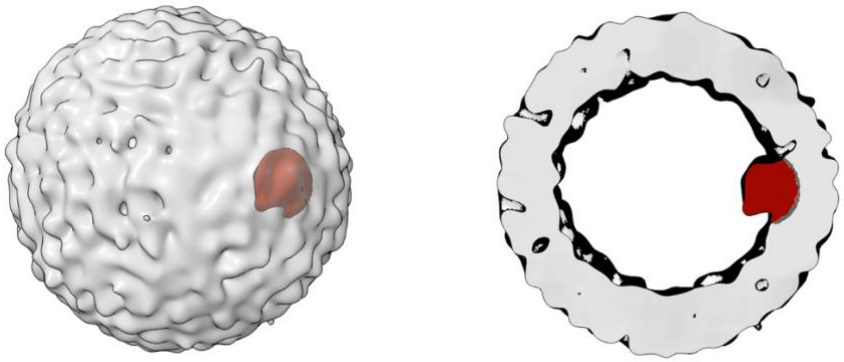

Figure 3. Reconstruction of iron oxide loaded ferritin. The ferritin shell (gray) and iron oxide nanoparticle (red) can be seen in the low-resolution reconstruction of the complex (full map left, cross-section right), however secondary structure could not be seen in the maps.

Single particle cryo-EM shows promise for the structural study of protein-nanoparticle complexes, however future improvements will be required to obtain high-resolution structures of the protein-inorganic interface. While the data collected on GroEL-PtNPs produced a structure using relatively standard procedures, there are several improvements to the workflow that could improve the final maps. For example, while the sizes of the PtNPs are small relative to the GroEL protein, their high contrast will still drive alignment during classification. When the nanoparticles are within the overall particle, this does not seem to have a large effect, as in the structure shown here for GroEL-PtNP. However, in this sample there are also GroEL-PtNPs where the nanoparticles are bound to the outside of the GroEL protein, and these particles were not able to be properly classified. Using masking algorithms that can identify and mask the nanoparticles in the full image or in the extracted particle stacks could allow the classification and reconstruction of these off-centered protein-nanoparticle complexes, as well as improve the quality of final reconstructions. This type of masking should also help to improve the map quality for samples

where the ratio of protein to nanoparticle size is smaller, as is the case for the ferritin-FeNP sample presented here. For ferritin, it appears that the nanoparticle significantly affects the averaging, which is clear in the 2D class averages (Fig S5), which do not show the expected secondary structure that is present when analyzing apoferritin. Application of 3D masking procedures to the nanoparticle in the ferritin reconstruction presented here has the potential to improve the quality of the reconstruction. Future work on HuLF-FeNPs and GroEL-PtNPs will focus on optimizing masking procedures to improve the quality and resolution of the 3D maps obtained from these samples. Another approach to improve the quality of the maps presented here is to collect more data to obtain a higher number of particles that are complexes of both protein and nanomaterial. Additionally, collecting data sets closer to focus, potentially with an energy filter, could help to reduce the effects of the nanoparticle on the reconstruction process, thereby facilitating higher resolution reconstructions. These future improvements to cryo-EM data collection and processing procedures, as well as others not discussed here, for the study of protein-nanomaterial complexes will improve the quality of final structures and will bring an important new structure-function insights into how biological molecules interact with inorganic materials.

Notes

The authors declare no competing financial interest.

Supporting Information

Additional details on sample preparation, data collection and processing can be found in the associated supporting information.

Acknowledgements

We acknowledge the support for this project from the Air Force Office of Scientific Research FA9550-18-1–0012 and the National Science Foundation DMR-1942084. We would like to acknowledge the use of the Titan Krios at the Eyring Materials Center at Arizona State University and the funding of this instrument by NSF MRI 1531991.

References

1. Jain, P. K.; Huang, X. H.; El-Sayed, I. H.; El-Sayed, M. A., Noble Metals on the Nanoscale: Optical and Photothermal Properties and Some Applications in Imaging, Sensing, Biology, and Medicine. *Accounts of Chemical Research* **2008,** *41* (12), 1578-1586.
2. Wang, L. F.; Yang, R. T., New sorbents for hydrogen storage by hydrogen spillover - a review. *Energy & Environmental Science* **2008,** *1* (2), 268-279.
3. Knecht, M. R.; Pacardo, D. B., Employing high-resolution materials characterization to understand the effects of Pd nanoparticle structure on their activity as catalysts for olefin hydrogenation. *Analytical and Bioanalytical Chemistry* **2010,** *397* (3), 1137-1155.
4. Nudelman, F.; Sommerdijk, N. A. J. M., Biomineralization as an Inspiration for Materials Chemistry. *Angewandte Chemie-International Edition* **2012,** *51* (27), 6582-6596.
5. Mayer, G.; Sarikaya, M., Rigid biological composite materials: Structural examples for biomimetic design. *Experimental Mechanics* **2002,** *42* (4), 395-403.
6. Sumper, M., Biomimetic patterning of silica by long-chain polyamines. *Angew Chem Int Ed Engl* **2004,** *43* (17), 2251-4.
7. Schuler, D.; Frankel, R. B., Bacterial magnetosomes: microbiology, biomineralization and biotechnological applications. *Appl Microbiol Biotechnol* **1999,** *52* (4), 464-473.
8. Zhou, W.; Swift, B. J.; Baneyx, F., A minimized designer protein for facile biofabrication of ZnS:Mn immuno-quantum dots. *Chem Commun (Camb)* **2015,** *51* (17), 3515-7.
9. Dai, H.; Choe, W. S.; Thai, C. K.; Sarikaya, M.; Traxler, B. A.; Baneyx, F.; Schwartz, D. T., Nonequilibrium synthesis and assembly of hybrid inorganic-protein nanostructures using an engineered DNA binding protein. *J Am Chem Soc* **2005,** *127* (44), 15637-43.
10. Tamerler, C.; Khatayevich, D.; Gungormus, M.; Kacar, T.; Oren, E. E.; Hnilova, M.; Sarikaya, M., Molecular biomimetics: GEPI-based biological routes to technology. *Biopolymers* **2010,** *94* (1), 78-94.
11. Coyle, B. L.; Zhou, W.; Baneyx, F., Protein-aided mineralization of inorganic nanostructures. In *Bionanotechnology: Biological Self-assembly and its Applications*, Rehm, B., Ed. 2013; pp 63-83.
12. Crookes-Goodson, W. J.; Slocik, J. M.; Naik, R. R., Bio-directed synthesis and assembly of nanomaterials. *Chem Soc Rev* **2008,** *37* (11), 2403-12.
13. Chiu, C. Y.; Li, Y. J.; Ruan, L. Y.; Ye, X. C.; Murray, C. B.; Huang, Y., Platinum nanocrystals selectively shaped using facet-specific peptide sequences. *Nature Chemistry* **2011,** *3* (5), 393-399.

14. Pacardo, D. B.; Sethi, M.; Jones, S. E.; Naik, R. R.; Knecht, M. R., Biomimetic Synthesis of Pd Nanocatalysts for the Stille Coupling Reaction. *Acs Nano* **2009,** *3* (5), 1288-1296.
15. Dickerson, M. B.; Sandhage, K. H.; Naik, R. R., Protein- and peptide-directed syntheses of inorganic materials. *Chem Rev* **2008,** *108* (11), 4935-78.
16. Baneyx, F.; Schwartz, D. T., Selection and analysis of solid-binding peptides. *Curr Opin Biotechnol* **2007,** *18* (4), 312-7.
17. Sarikaya, M.; Tamerler, C.; Jen, A. K.; Schulten, K.; Baneyx, F., Molecular biomimetics: nanotechnology through biology. *Nat Mater* **2003,** *2* (9), 577-85.
18. Weidner, T.; Castner, D. G., SFG analysis of surface bound proteins: a route towards structure determination. *Phys Chem Chem Phys* **2013,** *15* (30), 12516-24.
19. Seker, U. O.; Wilson, B.; Kulp, J. L.; Evans, J. S.; Tamerler, C.; Sarikaya, M., Thermodynamics of engineered gold binding peptides: establishing the structure-activity relationships. *Biomacromolecules* **2014,** *15* (7), 2369-77.
20. Donatan, S.; Sarikaya, M.; Tamerler, C.; Urgen, M., Effect of solid surface charge on the binding behaviour of a metal-binding peptide. *Journal of the Royal Society Interface* **2012,** *9* (75), 2688-2695.
21. Pandey, R. B.; Heinz, H.; Feng, J.; Farmer, B. L.; Slocik, J. M.; Drummy, L. F.; Naik, R. R., Adsorption of peptides (A3, Flg, Pd2, Pd4) on gold and palladium surfaces by a coarse-grained Monte Carlo simulation. *Phys Chem Chem Phys* **2009,** *11* (12), 1989-2001.
22. Heinz, H.; Farmer, B. L.; Pandey, R. B.; Slocik, J. M.; Patnaik, S. S.; Pachter, R.; Naik, R. R., Nature of molecular interactions of peptides with gold, palladium, and Pd-Au bimetal surfaces in aqueous solution. *J Am Chem Soc* **2009,** *131* (28), 9704-14.
23. Pacella, M. S.; Koo da, C. E.; Thottungal, R. A.; Gray, J. J., Using the RosettaSurface algorithm to predict protein structure at mineral surfaces. *Methods Enzymol* **2013,** *532*, 343-66.
24. Shaw, W. J., Solid-state NMR studies of proteins immobilized on inorganic surfaces. *Solid State Nucl Magn Reson* **2015,** *70*, 1-14.
25. Drobny, G. P.; Long, J. R.; Karlsson, T.; Shaw, W.; Popham, J.; Oyler, N.; Bower, P.; Stringer, J.; Gregory, D.; Mehta, M.; Stayton, P. S., Structural studies of biomaterials using double-quantum solid-state NMR spectroscopy. *Annu Rev Phys Chem* **2003,** *54*, 531-71.
26. Baio, J. E.; Weidner, T.; Baugh, L.; Gamble, L. J.; Stayton, P. S.; Castner, D. G., Probing the orientation of electrostatically immobilized Protein G B1 by time-of-flight secondary ion spectrometry, sum frequency generation, and near-edge X-ray adsorption fine structure spectroscopy. *Langmuir* **2012,** *28* (4), 2107-12.
27. Masica, D. L.; Ash, J. T.; Ndao, M.; Drobny, G. P.; Gray, J. J., Toward a structure determination method for biomineral-associated protein using combined solid- state NMR and computational structure prediction. *Structure* **2010,** *18* (12), 1678-87.
28. Braig, K.; Otwinowski, Z.; Hegde, R.; Boisvert, D. C.; Joachimiak, A.; Horwich, A. L.; Sigler, P. B., The crystal structure of the bacterial chaperonln GroEL at 2.8 Å. *Nature* **1994,** *371* (6498), 578-586.
29. Tang, Y.-C.; Chang, H.-C.; Roeben, A.; Wischnewski, D.; Wischnewski, N.; Kerner, M. J.; Hartl, F. U.; Hayer-Hartl, M., Structural Features of the GroEL-GroES Nano-Cage Required for Rapid Folding of Encapsulated Protein. *Cell* **2006,** *125* (5), 903-914.

30. Sennuga, A.; van Marwijk, J.; Boshoff, A.; Whiteley, C. G., Enhanced activity of chaperonin GroEL in the presence of platinum nanoparticles. *Journal of Nanoparticle Research* **2012,** *14* (5), 824.
31. Zheng, S. Q.; Palovcak, E.; Armache, J.-P.; Verba, K. A.; Cheng, Y.; Agard, D. A., MotionCor2: anisotropic correction of beam-induced motion for improved cryo-electron microscopy. *Nat Methods* **2017,** *14* (4), 331-332.
32. Grant, T.; Rohou, A.; Grigorieff, N., cisTEM, User-friendly software for single-particle image processing. *eLife* **2018,** *7*, e35383-e35383.
33. Theil, E. C.; Behera, R. K.; Tosha, T., Ferritins for Chemistry and for Life. *Coord Chem Rev* **2013,** *257* (2), 579-586.
34. Knovich, M. A.; Storey, J. A.; Coffman, L. G.; Torti, S. V.; Torti, F. M., Ferritin for the clinician. *Blood reviews* **2009,** *23* (3), 95-104.
35. He, D.; Marles-Wright, J., Ferritin family proteins and their use in bionanotechnology. *New Biotechnology* **2015,** *32* (6), 651-657.
36. Erickson, S. D.; Smith, T. J.; Moses, L. M.; Watt, R. K.; Colton, J. S., Non-native Co-, Mn-, and Ti-oxyhydroxide nanocrystals in ferritin for high efficiency solar energy conversion. *Nanotechnology* **2014,** *26* (1), 015703.
37. Iwahori, K.; Yoshizawa, K.; Muraoka, M.; Yamashita, I., Fabrication of ZnSe Nanoparticles in the Apoferritin Cavity by Designing a Slow Chemical Reaction System. *Inorganic Chemistry* **2005,** *44* (18), 6393-6400.
38. Vande Velde, G.; Rangarajan, J. R.; Toelen, J.; Dresselaers, T.; Ibrahimi, A.; Krylychkina, O.; Vreys, R.; Van der Linden, A.; Maes, F.; Debyser, Z.; Himmelreich, U.; Baekelandt, V., Evaluation of the specificity and sensitivity of ferritin as an MRI reporter gene in the mouse brain using lentiviral and adeno-associated viral vectors. *Gene Therapy* **2011,** *18*, 594.
39. Jacobs, J. F.; Hasan, M. N.; Paik, K. H.; Hagen, W. R.; van Loosdrecht, M. C. M., Development of a bionanotechnological phosphate removal system with thermostable ferritin. *Biotechnology and Bioengineering* **2010,** *105* (5), 918-923.
40. Pozzi, C.; Ciambellotti, S.; Bernacchioni, C.; Di Pisa, F.; Mangani, S.; Turano, P., Chemistry at the protein-mineral interface in L-ferritin assists the assembly of a functional (mu3-oxo)Tris[(mu2-peroxo)] triiron(III) cluster. *Proc Natl Acad Sci U S A* **2017,** *114* (10), 2580-2585.